



AIAA 99-1937
INLET NOISE REDUCTION BY
SHIELDING FOR THE BLENDED-
WING-BODY AIRPLANE

Lorenzo R. Clark and Carl H. Gerhold
NASA Langley Research Center
Hampton, VA 23681-2199

5th AIAA/CEAS Aeroacoustics Conference
May 10-12, 1999/Greater Seattle, Washington

For permission to copy or republish, contact the American Institute of Aeronautics and Astronautics
1801 Alexander Bell Drive, Suite 500, Reston, Virginia 20191-4344

INLET NOISE REDUCTION BY SHIELDING FOR THE BLENDED-WING-BODY AIRPLANE

Lorenzo R. Clark*
and Carl H. Gerhold†

Abstract

Noise shielding benefits associated with an advanced unconventional subsonic transport concept, the Blended-Wing-Body, were studied using a 4-percent scale, 3-engine nacelle model. The study was conducted in the Anechoic Noise Research Facility at NASA Langley Research Center. A high-frequency, wideband point source was placed inside the nacelles of the center engine and one of the side engines in order to simulate broadband engine noise. The sound field of the model was measured with a rotating microphone array that was moved to various stations along the model axis and with a fixed array of microphones that was erected behind the model. Ten rotating microphones were traversed a total of 22 degrees in 2-degree increments. Seven fixed microphones covered an arc that extended from a point in the exhaust exit plane of the center engine (and directly below its centerline) to a point 30 degrees above the jet centerline. While no attempt was made to simulate the noise emission characteristics of an aircraft engine, the model source was intended to radiate sound in a frequency range encompassing 1, 2, and 3 times the blade passage of a typical full-scale engine. In this study, the Blended-Wing-Body model was found to provide significant shielding of inlet noise. In particular, noise radiated downward into the forward sector was reduced by 20 to 25 dB overall in the full-scale frequencies from 2000 to 4000 Hz, decreasing to 10 dB or less at the lower frequencies. Also, it was observed that noise associated with the exhaust radiates into the sector directly below the model downstream to reduce shielding efficiency.

*Aerospace Engineer

†Sr. Research Engineer, Member, AIAA

Copyright © 1998 by the American Institute of Aeronautics and Astronautics, Inc. No copyright is asserted in the United States under Title 17, U.S. Code. The U.S. Government has a royalty-free license to exercise all rights under the copyright claimed herein for Governmental Purposes. All other rights are reserved by the copyright owner.

Nomenclature

D jet exit diameter
r microphone radius
X distance measured upstream from the exit plane of the center nacelle of the model
 θ microphone polar angle position
 ψ microphone azimuthal angle position

Introduction

A program was recently conducted by NASA and U. S. industry and universities to investigate pre-competitive payoff aeronautical concepts (See Ref. 1 for results from a related industry study.). One of the concepts studied in the program was the Blended-Wing-Body, also known as the BWB. The purpose of this effort was to assess the technical and commercial viability of an advanced unconventional subsonic transport. This unique transport concept simultaneously addresses far-term NASA goals for emissions, noise, capacity, safety, and cost of travel. The present paper focuses on noise-related aspects of the BWB. Specifically, the paper presents results from a test model that was performed in order to evaluate the wing noise shielding benefit of the upper surface engine installation. A schematic of the BWB model is given in Figure 1.

The BWB concept in this study has a design payload of 800 passengers, 7000 nautical-mile range, Mach 0.85 (about 560-mph) cruise speed, and utilizes technology levels expected for service in the 2020 timeframe. To minimize the required aircraft surface (wetted) area per passenger, the BWB combines a rigid, wide airfoil-shape fuselage with high aspect ratio wings and semi-buried engines. The design has two full passenger decks with a typical long-range, 3-class arrangement within a thick centerbody. The seating is laid out in five parallel single aisle compartments on each deck. Each compartment is approximately equivalent to a very short narrow body aircraft, and even though the passenger complement is relative high, the overall

egress paths for passengers are shorter than most large conventional configurations. The estimated takeoff gross weight of the aircraft is 823,000 pounds (about 3/4 composites, 1/4 metal), and it uses three 60,000-pound class turbofan engines. The engines are located on top of the wing, aft of the passenger compartment. This works well for balance, but also has several beneficial side effects. The turbines and compressors are completely clear of the main structural elements, pressurized compartments, and fuel, which can improve safety. The large fans on the high bypass-ratio engines are shielded from the ground by the centerbody, which will improve the noise characteristics for people on the ground. The latter benefit is the primary motivation for the study documented here.

Blended-Wing-Body Model

A photograph of the BWB model used in this work is shown in Figure 2. The circular hoop in the foreground is a microphone boom that will be discussed in the next section. The model is a 4 percent scale version of the BWB concept described in the introduction. The model, which is made of a fiberglass resin, has a wing span of 11.6 ft. and is 6.4 ft. from the tip of the nose to the jet exit plane of the center engine. Figure 3 is a side view of the model and reveals the location at which the model was fastened to a vertical sting.

Facility and Experimental Set-Up

The experiment was conducted in the Anechoic Noise Research Facility (ANRF) at NASA Langley Research Center. The internal dimensions of the test area (inside wedge tips) are 28 ft. by 27 ft. by 24 ft. The walls are covered with acoustic wedges which are 3 ft. thick and yield an absorption coefficient above 99 percent above a frequency of 100 Hz. A more detailed description of the ANRF is given in Reference 2. The BWB model was mounted on a vertical post in a corner of the facility. This allowed for positioning of a microphone boom (circular hoop) that was moved along a track on the floor of the test chamber. The boom was used for most of the acoustic data acquisition.

A microphone traverse system is a key part of the facility, and it allows for axial and azimuthal traverses. The circular hoop is mounted on a sled that can move in the axial direction on the ground track. In the present test, boom microphones used for data collection were installed on rods that moved

parallel to the model axis as shown in Figures 2 and 3. Although the boom was equipped with sixteen equally spaced microphones, only the ten that are numbered in Figure 4a (end view) were used. These microphones were rotated up to 22 degrees in the azimuthal direction during the data collection process. Rotations were made in 2-degree increments, which allowed for high resolution in the azimuthal direction. Figure 4b is a side view of the microphone boom. The rod-mounted microphones were positioned at axial stations ranging from $X/D = 0$ at the jet exit plane of the center engine to $X/D = 13.5$, a point near where the wing leading edge transitions to the BWB centerbody. The actual station locations in inches were at $X = 0, 4, 8, 24, 42, 48$ and 54 . Acoustic foam was installed on the ground track and the hoop in order to minimize sound reflections in the test chamber. For this reason, the axial positions of the boom had to be set manually. However, the azimuthal traverses were driven by a stepper motor with precision of more than 1/100th of an inch.

In addition to the movable hoop array, a fixed array was located behind the model. This array consisted of seven microphones on a 27-inch radius (6-3/4 nacelle diameters) in a vertical plane centered on the center engine nozzle exit. The microphones covered noise emission angles from 90 degrees, θ_{ref} , which is on the plane of the nozzle exit, to a point 30 degrees above the nozzle centerline. The fixed microphone array can be seen clearly in Figure 3 and is shown schematically in Figure 5.

Also visible in Figure 3 is hardware that was used to stabilize the point source inside the exhaust end of the center engine nacelle. A close-up view of the actual source, consisting of four impinging air jets, is shown in Figure 6a. The impinging jet noise source is designed to provide a high-intensity, high-frequency, point noise source for this experiment. It was found to provide sound at least 10 dB above the noise floor at frequencies up to 100,000 Hz. A spectrum of the noise source at a point directly over it ($X/D = 0, \psi = 90$ degrees) is shown in Figure 6b.

Instrumentation and Data Analysis

The acoustic sensors mounted on the circular hoop were 10 Bruel and Kjaer 1/2-inch diameter microphones; 1/4-inch microphones were used with the stationary array. Noise measurements were acquired on a multiple channel data acquisition

system set to collect 4 seconds of data at 250,000 samples per second simultaneously from 17 microphone channels. The data were band pass filtered with a passband from 3 kHz to 100 kHz. This passband corresponds to 120 Hz and 4 kHz, respectively, in the full scale. Sound spectra were scaled in frequency based on the model physical scale factor, and the resulting narrow band data were converted to one-third octave sound spectra.

Description of Experiment

Acoustic measurements were made around the model with the point source in three configurations: source alone, source in an isolated nacelle, and source in a nacelle of the BWB model. In the second case, a 19-1/4 inch section of metal pipe with a 4-inch inside diameter served as the engine nacelle. The configurations tested with the source and center nacelle are summarized in Table 1. Source in the nacelle configurations consisted of the source entering the nacelle through the exhaust plane. Radiated sound spectra obtained with the source in the BWB model nacelle were subtracted from spectra obtained with the source in the isolated nacelle to determine the insertion loss of the wing (noise shielding).

Microphone data were taken with the center of the impinging jets located at the center of the center nacelle; data were also taken with the source at the center of one of the side engine nacelles of the BWB model. The pipe that represented the isolated nacelle case was tested with the BWB model removed from the anechoic chamber. The pipe occupied the same location that the center engine nacelle occupied when it was tested. The noise source was at the center of the pipe during acoustic data collection. A microphone traverse was also made with the source alone at the location of the center of the center engine nacelle. The purpose of this test was to assess the desired omni-directive characteristics of the impinging jets noise source.

Results

The acoustic data collected for this experiment were reduced to the three tones 1st harmonic (fundamental), 2nd harmonic, and 3rd harmonic, and the overall sound pressure level (OASPL) for the broadband after the tones were removed. The harmonics corresponded to source frequencies of 12.5 kHz, 25.0 kHz, and 37.5 kHz, respectively. The harmonics are similar to what fan tones would be at

1, 2, and 3 times the blade passage frequency. For each measurement along the model axis the test data were analyzed as model insertion loss (noise shielding) in sound pressure level (SPL) over the full-scale frequency range 120 Hz to 4 kHz. The data were also analyzed as contour plots that gave noise as a function of azimuthal angle and microphone measurement location. The limited amount of data presented in this paper gives typical results for the experiment.

Directivity of the Noise Source Alone

Figure 7 is a contour plot that shows OASPL variation above and below the impinging jets noise source. As the figure indicates, noise symmetry is very much in evidence above and below the source. Above the source the noise varies from 80 to 84 dB on average. There is somewhat less noise variation below the source. The average noise level in this region is 80 to 82 dB.

Noise Measurements with BWB Model Present and Source in Center Nacelle

Noise contours above and below the model are given in Figure 8 for the BWB with the source in the center engine. The data in Figure 8a were obtained with the sound plug out and Figure 8b shows data that were obtained with the sound plug in the nacelle inlet. The data in Figures 8a and 8b are for the case involving the 1st harmonic.

Since the data in Figure 8a were measured without the sound plug installed, both exhaust noise and inlet noise are shown in the plot. Upon initial examination, it is obvious that considerable shielding of the inlet noise is accomplished beneath the wing. However, in order to examine the figures in more detail, it is convenient to focus one's attention first on the aft sector (X less than 27 inches) and then on the forward sector (X greater than 27 inches).

If average aft noise (40-42 dB) below the model is compared with average aft noise (42-44 dB) above the model, average shielding of about 2 dB is found to occur. This is not unexpected, since the nacelle exhaust exit plane protrudes past the trailing edge of the wing, affording virtually no shielding in the aft direction. However, examination of the forward sector finds average levels of 36-38 dB below the model that compare to levels of 56-60 dB above the model. The noise shielding that results is approximately 22 dB.

Figure 8b provides an opportunity to look at noise measured above and below the model for the situation where only exhaust noise was radiated from the nacelle. Therefore, inlet noise was not a factor in this instance. If compared with the data previously given in Figure 8a, noise shielding in the forward sector is similar. However, shielding in the aft sector is increased by approximately 8 dB. Although this model configuration is unrealistic, the results in Figure 8b suggest that engine inlet noise associated with the aft sector has the effect of limiting the noise shielding benefit in the vicinity of the engine exhaust.

Measurements obtained behind the model using the stationary microphones are not presented in the present paper, but they indicated that when engine inlet and exhaust noise are present, noise shielding behind the model is non-existent.

Noise Shielding Associated with BWB Model

The contour plots in Figure 9 indicate the effect of the BWB model on noise generated by the center nacelle with source in exhaust and sound plug out. The plots were obtained by subtracting the noise of Configuration 2 from the noise of Configuration 3 (See Table 1.). In this figure, distance is given in numbers of jet diameters, X/D . It is seen that wide variation of the noise difference occurs above and below the model. Data associated with the fundamental tone are given in Figure 9a. As expected, noise level increases are generally observed above the model. This is primarily a result of the nacelle inlet noise interacting with the upper surface of the wing. These noise increases range from 6 dB in the aft region to 10 dB in the forward region. Below the model noise shielding is considerably greater in the forward sector. Here the shielding ranges to as high as 22 dB, but smaller values are typical. In the aft sector maximum noise shielding is about 6 dB.

Sound pressure data are presented in Figures 9b and 9c for the 2nd harmonic and 3rd harmonic tones, respectively; OASPL data are shown in Figure 9d. The results of the first two figures serve to indicate that noise shielding beneath the model is slightly better in the forward sector at the 3rd harmonic, but all three figures show similarly high levels of shielding. This is predictable though, since the wing shielding mechanism works best for relatively high-frequency, short-wavelength noise, as is present in all three cases. In figure 9d the most noticeable

feature is that the OASPL noise is more uniformly distributed throughout the sound field than was the tone noise, and fewer noise fluctuations above and below the model are seen to occur.

Figure 9e is presented as a complementary figure to Figures 9a-9d. It too compares data taken with the nacelle alone and the full configuration. In this figure SPL is plotted versus scaled frequency. Noise reductions of as much as 23 dB occur over the full-scale frequency range of 0 to 4kHz.

Estimated Noise Shielding for All Engines

The estimated effect of the BWB model on noise shielding at the 3rd harmonic when all three nacelles have noise sources in the exhausts is shown in Figure 10. As previously mentioned, acoustic measurements were obtained with the noise source in one of the side engine nacelles. In fact, data were taken with and without the BWB model in place, in order to determine the noise contribution of the side nacelle. By adding to these measurements an equivalent amount of noise, the acoustic effect of the second side engine could be accounted for. The noise data of both side engines were subsequently added to the center nacelle data to give the Figure 10 results. With the 3-engine configuration, noise shielding below the model is in excess of 20 dB in the forward sector. This is reflected in Figure 10a where 3rd harmonic data are presented and in Figure 10b where OASPL data are shown. Maximum noise shielding in the aft sector is only about 10 dB relative to both the 3rd harmonic and OASPL data.

Conclusions

This report documents the first known experimental acoustics study conducted to investigate inlet noise shielding associated with a 3-engine Blended-Wing-Body model. The following conclusions are drawn from the study:

1. Significant reduction of engine noise is obtainable beneath the model. For a mode where all three engines are operating, noise shielding in excess of 20 dB is possible in the forward sector of the model.
2. The greatest amount of noise shielding in the forward sector occurs for the 3rd harmonic tone.
3. Maximum noise shielding (on the order of 10 dB) in the aft sector of the model is relatively smaller than that in the adjacent forward sector.

Both exhaust and inlet radiated noise contribute to this result.

Acknowledgments

The authors are extremely grateful for contributions made to the success of this project by Larry Becker, Ahmad Naser, and Timothy Lavalley of Lockheed-Martin.

References

1. The Boeing Company, Long Beach, CA, "Blended-Wing-Body Technology Study," Final Report No. CRAD-9405-TR-3780, prepared for NASA-Langley Research Center under NAS1-20275, October 1997.
2. Hubbard, Harvey H.; and Manning, James C., "Aeroacoustic Research Facilities at NASA Langley Research Center," NASA TM 84585, March 1983.

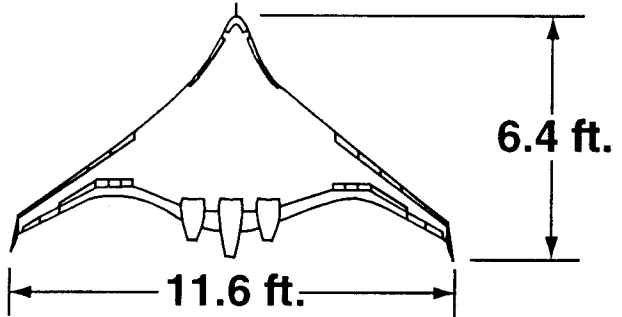


Figure 1. Schematic of BWB model.

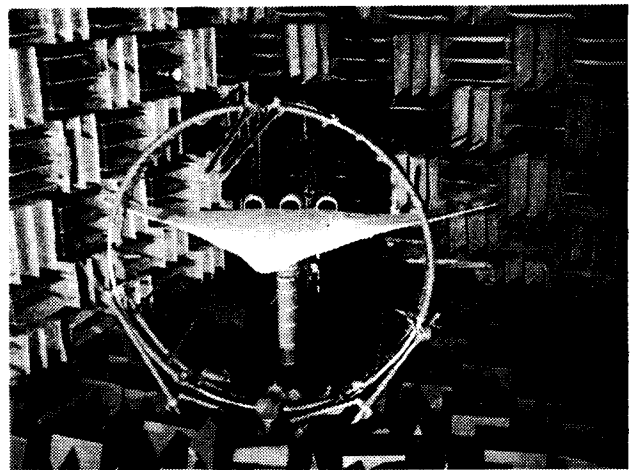


Figure 2. Photo of BWB model in anechoic noise facility (frontal view).

Table 1. Configurations tested

<u>Configuration number</u>	<u>Depiction</u>	<u>Description</u>
1		Noise source only
2		Source in isolated nacelle exhaust (E), sound plug out, center engine nacelle
3		Source in BWB nacelle exhaust, sound plug out, center and side engine nacelles

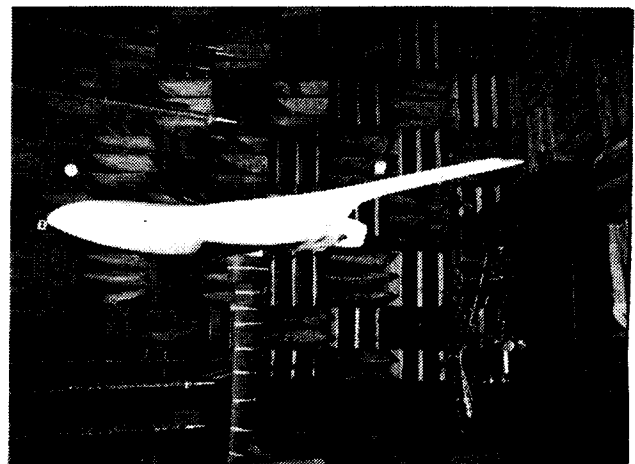
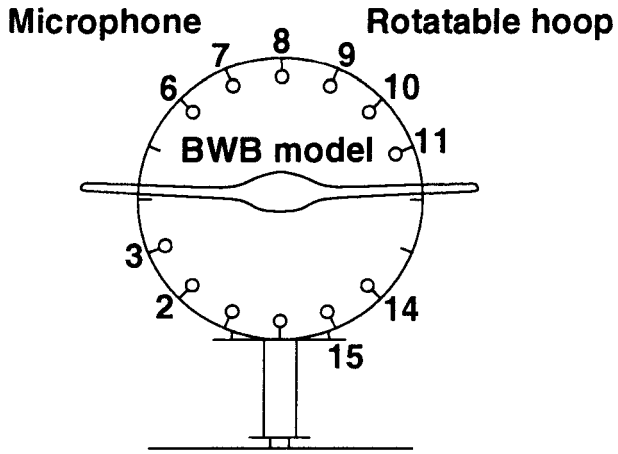
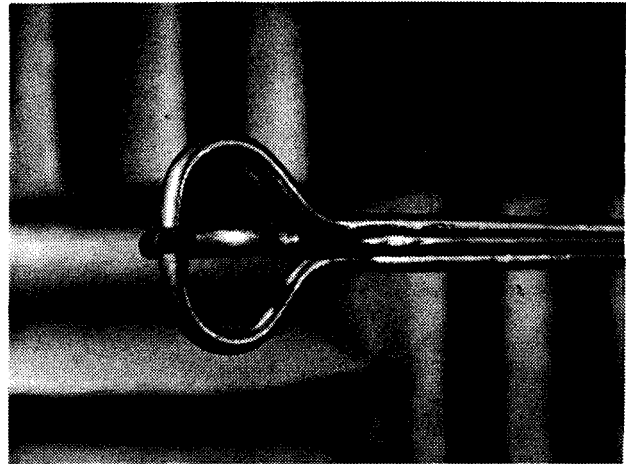


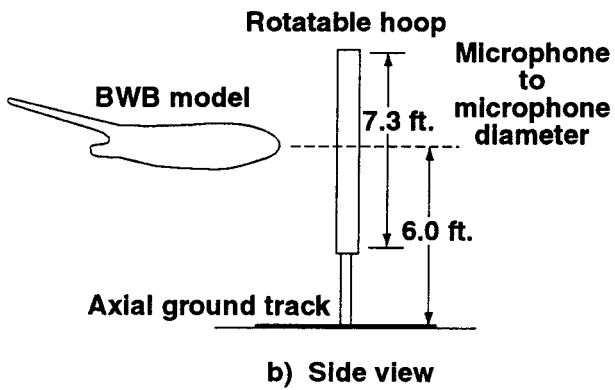
Figure 3. Photo of BWB model in anechoic noise facility (side view).



a) End view



a. Photo of point source consisting of four impinging air jets.



b) Side view

Figure 4. Rotatable microphone hoop.

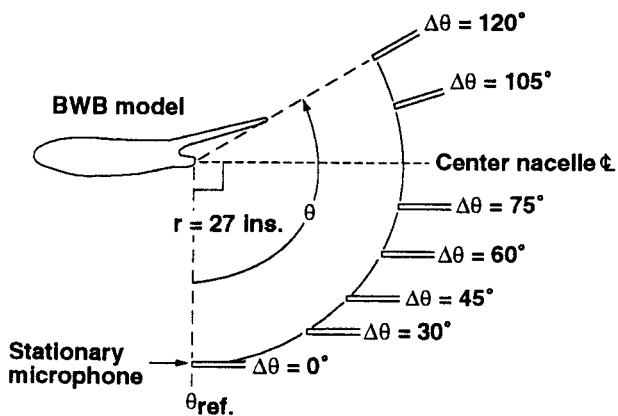
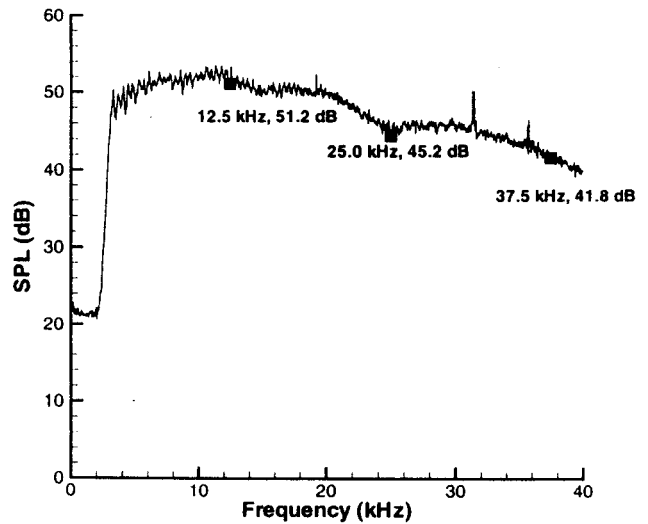


Figure 5. Schematic of fixed microphone array.



b. Spectrum of noise source, $\psi = 90^\circ$, $X/D = 0$.

Figure 6. Photo of point source consisting of four impinging air jets; spectrum of noise source for $\psi = 90^\circ$ and $X/D = 0$.

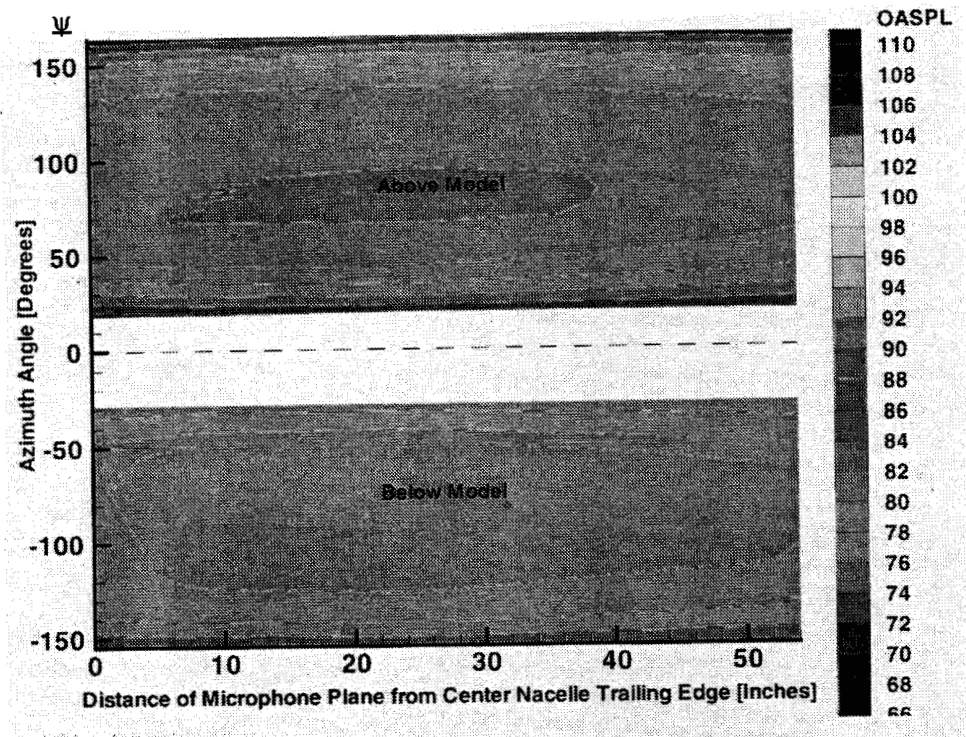
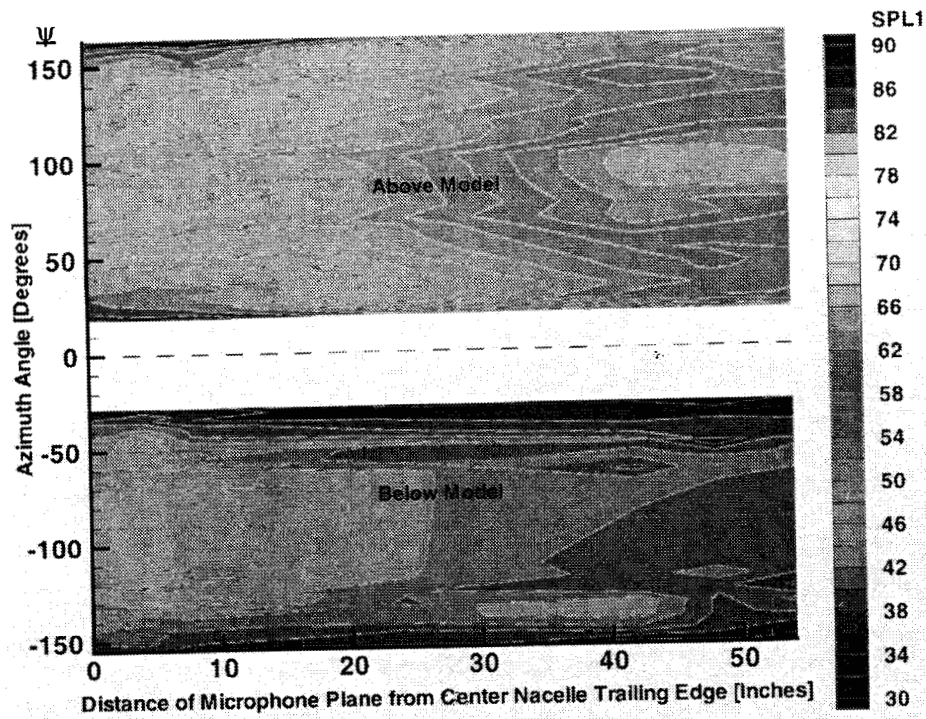
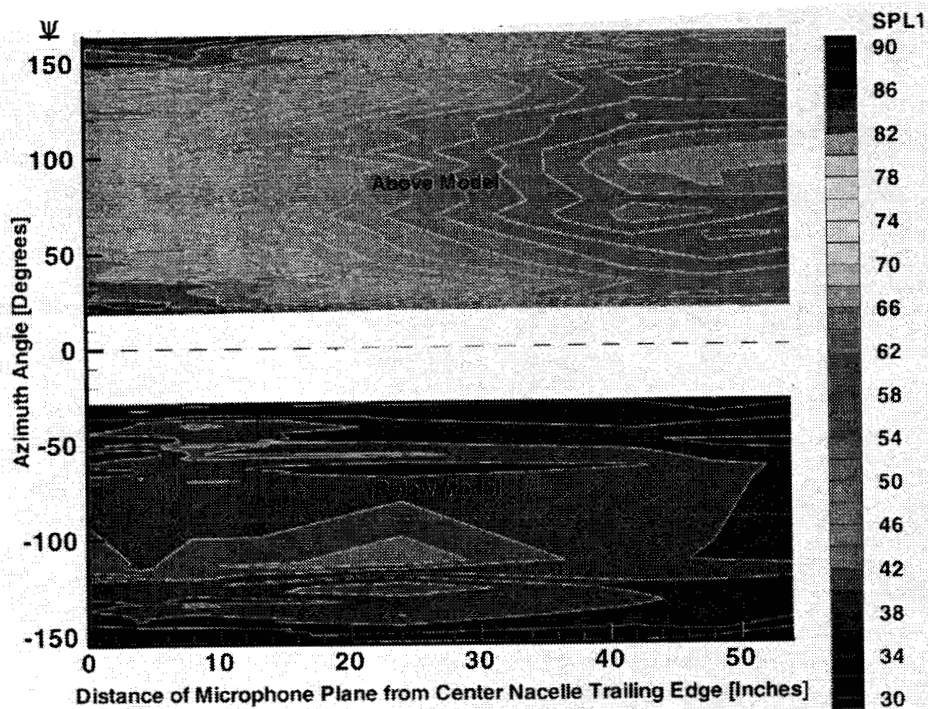


Figure 7. Contour plot showing noise field above and below the noise source alone.

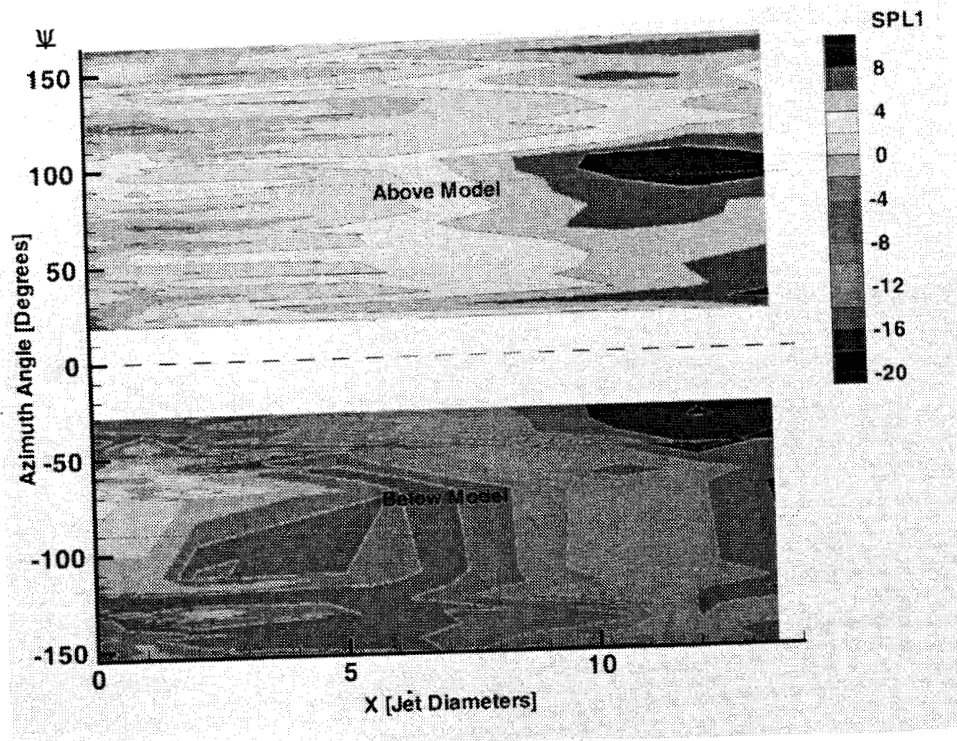


a. Sound plug out.

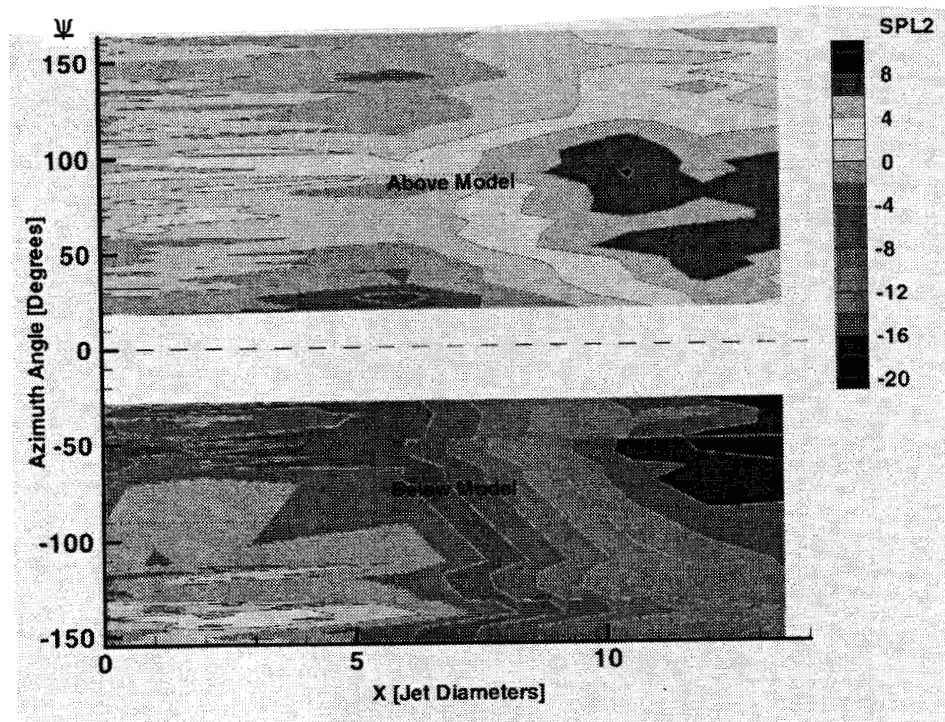


b. Sound plug in.

Figure 8. Contour plots obtained with model in place, noise source in jet of center engine nacelle, 1st harmonic; sound plug out; sound plug in.

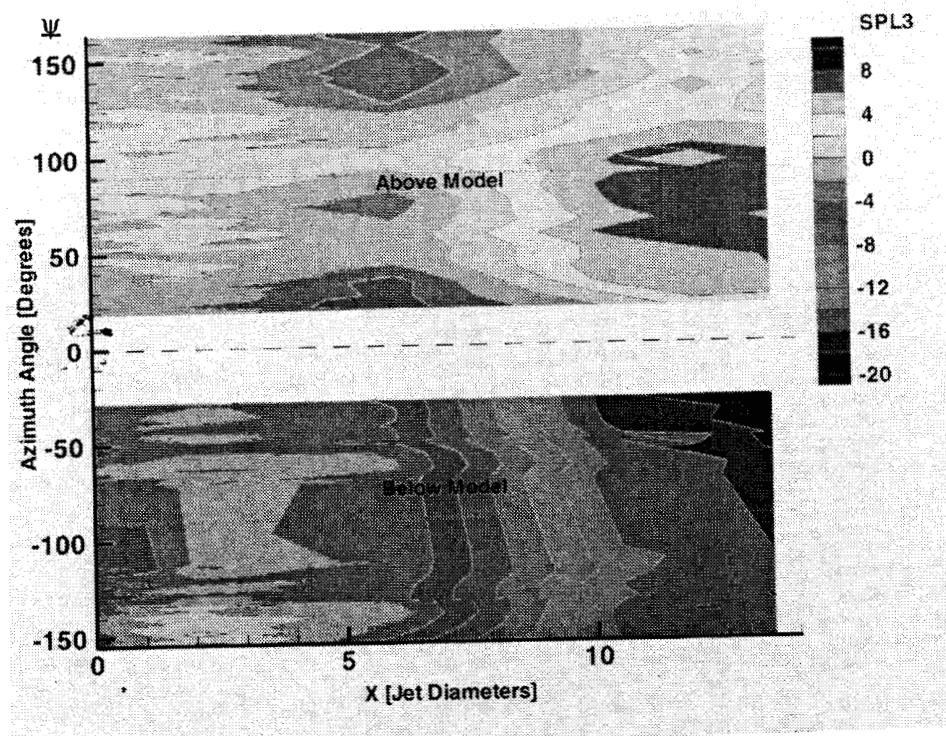


a. 1st harmonic.

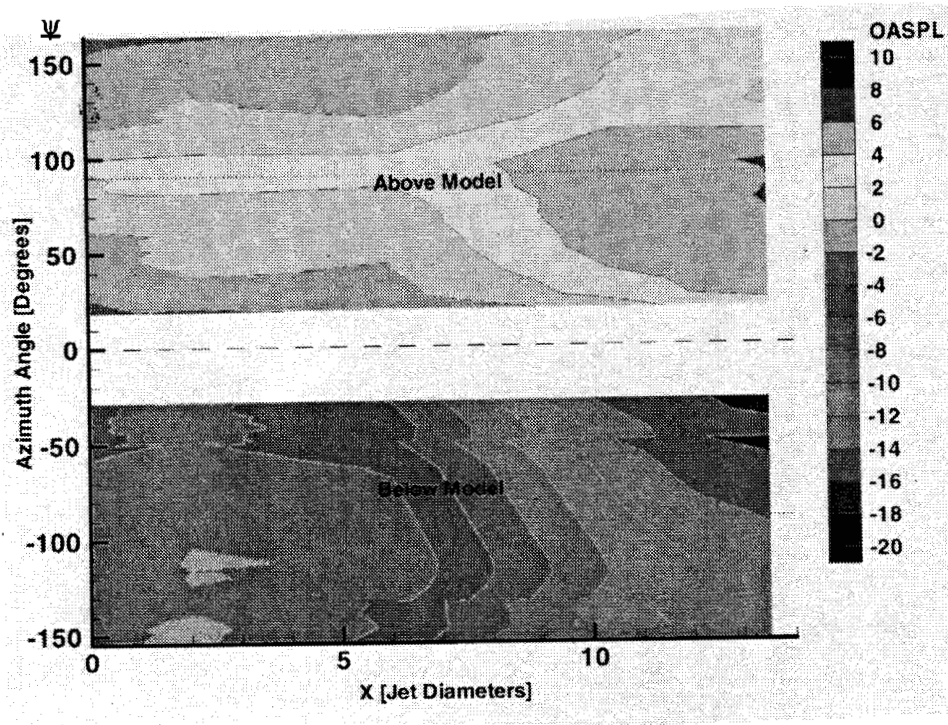


b. 2nd harmonic.

Figure 9. Noise contours of Configuration 4 minus noise contours of Configuration 2; SPL versus scaled frequency in forward sector below model.

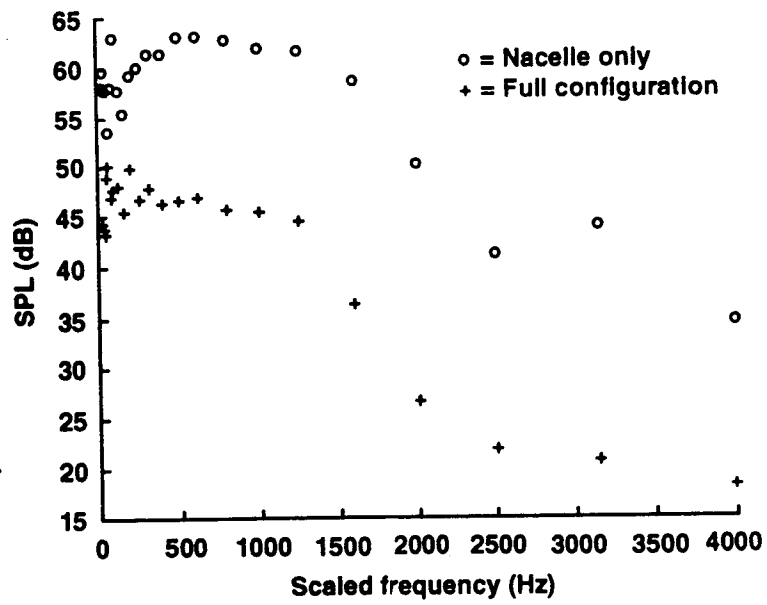


c. 3rd harmonic.



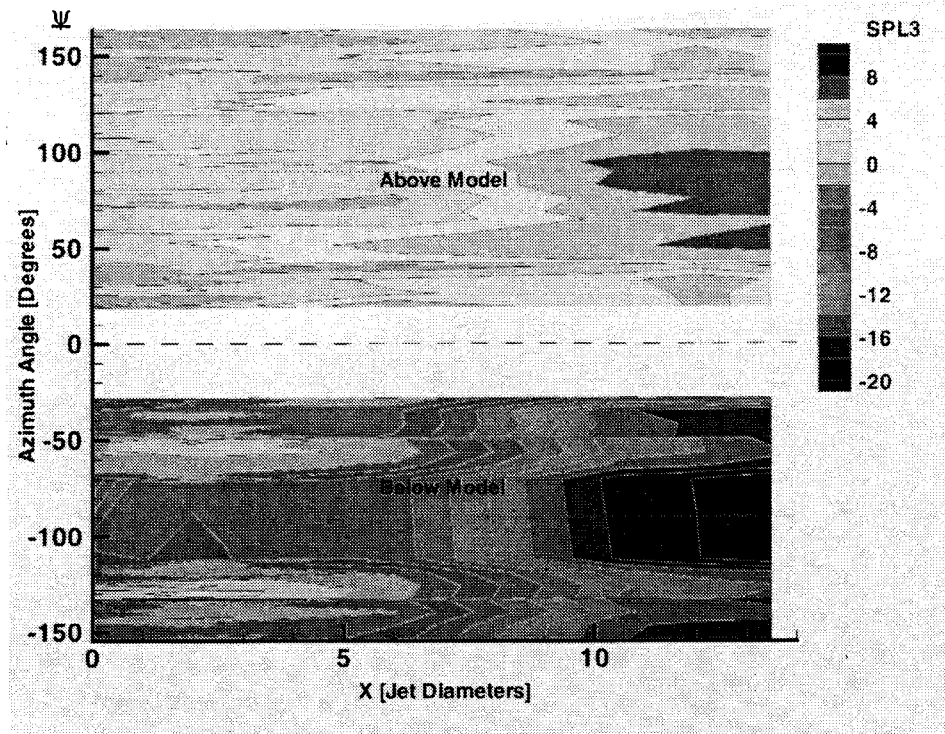
d. OASPL.

Figure 9. Continued.

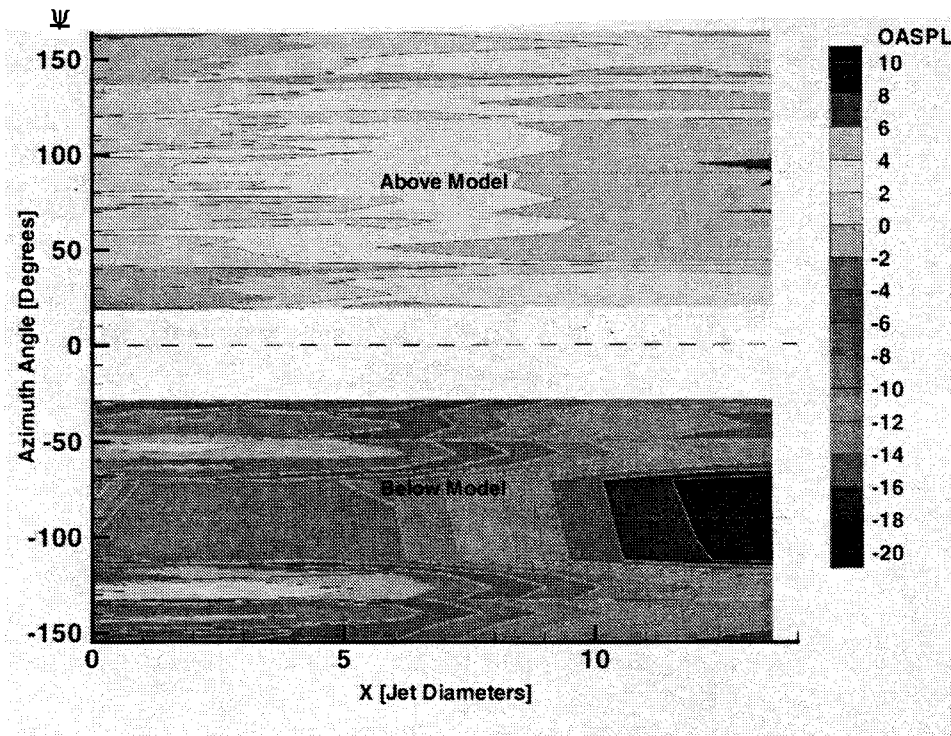


e. Spectrum.

Figure 9. Concluded.



a. 3rd harmonic.



b. OASPL.

Figure 10. Estimated noise shielding for source in all three engine nacelles and sound plug out; 3rd harmonic; OASPL.